



Thermodynamic Analysis for the Solubility of Allopurinol in Aqueous and Non-aqueous Mixtures at Various Temperatures

M. Ángeles Peña¹ · Ana B. Sánchez¹ · Begoña Escalera¹ · Abolghasem Jouyban^{2,3} · Fleming Martínez⁴

Received: 11 April 2022 / Accepted: 17 June 2022 / Published online: 11 July 2022
© The Author(s) 2022

Abstract

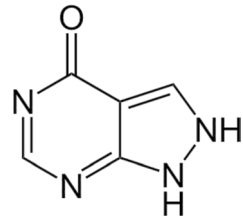
The solubility of allopurinol was measured at several temperatures (15–35 °C) in ethanol–water, ethanol–ethyl acetate, and ethyl acetate–hexane mixtures. The mole fraction solubility shows two solubility maxima against the co-solvent (ethanol) ratio (70 % ethanol–water and 100 % ethyl acetate) at each of the five temperatures studied. The authors correlated the solubility data in binary solvent mixtures at various temperatures using a modified version of the Jouyban–Acree model. The respective apparent thermodynamic functions Gibbs energy, enthalpy, and entropy of solution were obtained from the solubility data through the van't Hoff equations. The apparent enthalpies of solution are endothermic and display a maximum at 20 % ethanol in water, as ethanol is added to water, the entropy of the system increases. In the non-aqueous mixture (ethanol–ethyl acetate), enthalpy is the driving force throughout the whole solvent composition. An enthalpy–entropy compensation analysis confirms a non-linear enthalpy–entropy relationship in plots of enthalpy vs. Gibbs energy of solution, i.e., two different mechanisms involved in the solubility enhancement. An inverse Kirkwood–Buff integral analysis of the preferential solvation indicated that in ethanol-rich mixtures, the drug is preferentially solvated by water, and it is acting mainly as a Lewis base in front to water.

Keywords Allopurinol · Solubility profiles · Solubility mathematical model · Enthalpy–entropy compensation · Thermodynamic functions · Solvation

✉ M. Ángeles Peña
angeles.pena@uah.es

Extended author information available on the last page of the article

Fig. 1 Chemical structure of allopurinol



1 Introduction

Solubility mathematical models can be successfully developed for predicting drug solubility in such solvent mixtures, thus allowing reduction of the number of expensive and time-consuming experiments required during pre-formulation studies [1–6]. In this work, we in-depth investigated the behavior of allopurinol in several solvent mixtures, in order to test the influence of medium and polarity of the co-solvents selected (solubility parameters δ_1 from 14.93 MPa^{1/2} to 47.8 MPa^{1/2}). Data in solvent mixtures have served to test the prediction models for non-polar solutes in non-aqueous solvent mixtures [7–11]. Aqueous mixtures are of particular interest for pharmaceutical industry. Low solubility causes important problems to design liquid dosage forms and lowers drug bioavailability.

Thermodynamic functions provide a better understanding of the driving force of the solution process, the variation of the heat of solution (ΔH_2^S) with solvent composition has been used to explain the origin of the solubility enhancement by co-solvents [12–15]. Henceforth, the subscript 2 refers to the solute and the 1 to the solvent in all parameters. Enthalpy–entropy compensation analysis was also suggested as a tool to identify changes of the dominant mechanism that controls the co-solvent action [16–20].

Krug [21] showed that this kind of plots might only reflect a statistical compensation instead of a true chemical compensation effect because the errors of the slope and the intercept estimates are correlated. The errors are uncorrelated when ΔH_2^S is plotted against the ΔG_2^S values obtained at harmonic mean of the experimental temperature (T_{hm}). Using this procedure found for the first time an enthalpy–entropy compensation for the solubility of a drug molecule (phenacetin) in aqueous mixtures of water–dioxane. The relationship was non-linear. New non-linear compensation relationships were then found for other drugs in ethanol–water mixtures [12, 13, 22, 23]. The analyses of extrathermodynamic relationship, correlation between ΔH_2^S and ΔG_2^S , are research tools in pharmaceutical and biochemical science. That analysis allows checking the usefulness of this kind of study that controls the co-solvent action.

Allopurinol is a 1H-pyrazolo[3,4-d]pyrimidin-4(2H)-one, and it is used mainly to treat hyperuricemia and its complications, including chronic gout. It is a xanthine oxidase inhibitor, which is administered orally. It works by reducing the production of uric acid in the body. High levels of uric acid may cause gout attacks or kidney stones (Fig. 1).

2 Experimental Section

Different aqueous and non-aqueous binary mixtures have been prepared by using Lewis base (ethyl acetate and hexane) and amphiprotic co-solvents (ethanol and water) at various temperatures (15–35 °C). The temperature range studied was selected to include the physiological temperature by using a small extrapolation and also those variations that may occur during the storage of liquid dosage forms. In our knowledge, no data in solvent mixtures for this drug are found in the literature.

2.1 Reagents and Materials

Allopurinol (mass fraction purity: 0.995) was kindly provided by Sigma-Aldrich (Germany). This product was anhydrous, as tested with the Karl–Fisher method. The solvents used were ethyl acetate, ethanol, and hexane (spectrophotometric grade, Panreac, Monplet and Esteban, Barcelona, Spain) and double-distilled water. The different solvent binary mixtures were prepared by volume. The detailed description of the chemicals used in the experiment is listed in Table 1.

2.2 Solubility Measurements

Sealed flasks containing an excess of drug powder in the presence of a fixed volume of pure solvent or solvent mixture were shaken in a temperature-controlled bath (35 ± 0.1 °C, Heto SH 02/100, Germany) until reaching the equilibrium. The dissolution curves versus time were studied in every pure solvent and the different binary mixtures. The solid phase at equilibrium was removed by filtration (Durapore membranes, 0.2 µm pore size). The drugs did not significantly adsorb onto the membranes. The samples were diluted with ethanol 96 % v/v and spectrophotometrically assayed (Shimadzu UV-2001PC, Japan). The range of linear response and the maximum absorption wavelengths used were 2–7 µg/mL and 209 nm. Dilution ratio for the spectroscopic analysis was more than 100 times in all cases, so the effect of the other solvents on extinction coefficients is negligible. Pipettes and filter devices were

Table 1 Source and purities of the compound used in this research

Compound	CAS	Formula	Molar Mass (g·mol ⁻¹)	Source	Purity in mass fraction ^a
Allopurinol	315–30-0	C ₅ H ₄ N ₄ O	136.112	Kindly supply Laboratories Normon SA	0.96
Ethanol	64–15-5	C ₂ H ₆ O	46.07	Panreac	0.995
Ethyl acetate	141–78-6	C ₄ H ₈ O ₂ /CH ₃ COOC ₂ H ₅	88.10	Panreac	0.995
Hexane	110–54-3	CH ₃ CH ₂ CH ₂ CH ₂ CH ₂ CH ₃	86.18	Panreac	0.995
Water		H ₂ O	18.02	Obtained by distillation	<0.999

^aAs stated by the supplier

maintained at the appropriate temperature inside a thermostated incubator (Raypa FKS 1800, USA). The densities of the solutions were measured at each temperature in 10-mL pycnometers, to convert the molar solubility into mole fraction units. All the experimental results were the average of at least three replicated experiments. The coefficient of variation [$CV = SDX_2/X_{2\text{mean}} \times 100$] was within 1.5 %.

2.3 Differential Scanning Calorimetry (DSC)

About 5 mg of samples of the original powder was placed in sealed aluminum pans under nitrogen purge (Mettler TA 4000, Mettler-Toledo, Greifensee, Switzerland). A single heating cycle was used in the 30–350 °C temperature range at a heating rate of 5 °C·min⁻¹. The DSC apparatus was calibrated with indium ($T_f = 156.6 \pm 0.2$ °C (onset); $\Delta H_f = 28.55 \pm 0.2$ J/g) using the same conditions of the drug samples. The fully automated evaluation performs a validation which compares the measured values with literature values. If, as in this case, the values are within the allowed limits, it is within the specifications. The thermal effects were measured at a heating rate of 5 °C·min⁻¹ under atmosphere of nitrogen (40 mL·min⁻¹). DSC analyses were also performed on samples of drug solid phases at equilibrium with saturated solutions in both pure solvents and solvent binary mixtures; the solid phases were removed by filtration and dried at room temperature, since treatment that is more drastic could eliminate solvent weakly bound to the crystal. Comparison of the thermograms allows to test whether the solvent mixtures affect the solid phase.

2.4 Hot Stage Microscopy (HSM)

An Olympus BX-50 (Japan) microscope connected to a HFS 91 hot stage and a temperature controller was used to observe the solid phase behavior before and after equilibration with the saturated solutions under polarized light at a heating rate of 5 °C·min⁻¹. Thermal microscopy permits the study and the physical characterization of materials as a function of temperature and time.

3 Results and Discussion

3.1 Characterization of the Solid State and Solubility Properties of the Original Powders: DSC and HSM Studies

Original powder shows a single endothermic effect related to melting point (Fig. 2). The onset and the heat of fusion of allopurinol were $T_f = 380.0 \pm 0.2$ °C and $\Delta H_f = 48.30$ kJ/mol (4.8 mg), respectively. In this work the onset is used instead of the melting point because in this way the influence of the mass is eliminated. The shoulder may indicate the presence of more than one crystal form within the sample. To rule out that does not exist decomposition, a wide number of DSC heating–cooling–heating experiments were performed with different maximum temperatures. The exothermic results in the cooling segment are due to solidification/

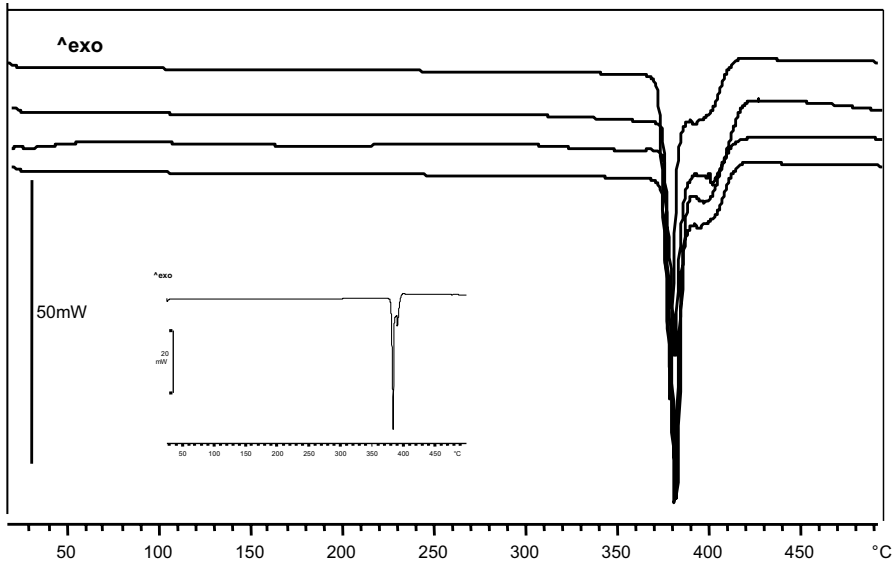


Fig. 2 DSC profile of allopurinol. 30 % water–ethanol, 20 % ethyl acetate–hexane, 100 % water, 50 % ethanol–ethyl acetate (up to down)

crystallization of the one of the melted crystals. Melting point therefore has an influence on solubility; a drug very soluble has fewer melting points than another insoluble. The thermograms of the solid phases after equilibration with the solvents did not show new thermal effects; in all cases, it is observed the same profile. The heat and temperatures of fusion did not significantly differ from the values found for the original powders in a wide range of temperature of 30 °C–350 °C, i.e., the thermal properties are not changed by the solvent (Fig. 2 and Table 2). The thermal behavior observed by HSM study indicated that the solid phases of allopurinol after equilibration with each saturated solutions in the different solvent mixtures employed remained unchanged, and it was in agreement with the DSC results.

3.2 Relationship Between Drug Polarity and the Solubility Profile

Figure 3 illustrates the solubility curves obtained against the polarity of the binary liquid systems, represented by the solubility parameters of Hildebrand (δ_1). The

Table 2 Temperature (T_f) and enthalpy of fusion (ΔH_f) of the solid phase equilibrated with saturated solutions in pure solvents selected

Solvent	T_f (°C)	ΔH_f (kJ·mol ⁻¹)
Water	382.41	48.852
Ethanol	382.54	41.889
Ethyl acetate	353.20	45.660
Hexane	383.45	47.865

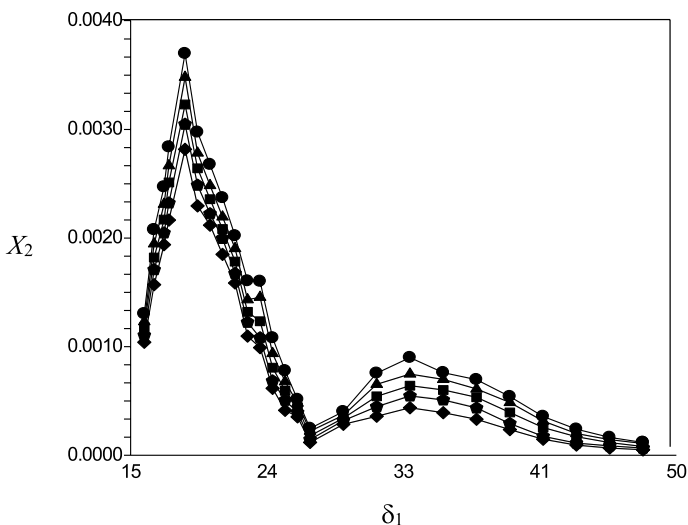


Fig. 3 Solubility mole fraction in ethanol–water ($\delta_1 = 26.51\text{--}47.97 \text{ MPa}^{1/2}$), ethanol–ethyl acetate ($\delta_1 = 26.51\text{--}18.49 \text{ MPa}^{1/2}$), and ethyl acetate–hexane ($\delta_1 = 18.49\text{--}14.93 \text{ MPa}^{1/2}$) mixtures at 35 °C (●), 30 °C (▲), 25 °C (■), 20 °C (◆) and 15 °C (◇)

solubility parameter is the cohesive energy density between compounds, and it is a physical and chemical parameter that is inherent to a substance, which is frequently used in the formulation design, chemical additive distribution, solvent selection, and membrane penetration [1, 12]. This parameter can be calculated for a binary mixture from the following expression ($\delta_1 = 18.49 \text{ MPa}^{1/2}$ for ethyl acetate, $\delta_1 = 26.51 \text{ MPa}^{1/2}$ for ethanol, $\delta_1 = 14.93 \text{ MPa}^{1/2}$ for hexane, and $\delta_1 = 47.86 \text{ MPa}^{1/2}$ for water), the volume fractions, ϕ_i and ϕ_j , of each component in the mixture, and the solubility parameters, δ_i and δ_j , of each fraction in the mixture:

$$\delta_1 = \phi_i \delta_i + \phi_j \delta_j \quad (1)$$

The experimental mole fraction solubility at 15–35 °C is included in Tables 3, 4, and 5, and solubility increases with temperature in aqueous and the non-aqueous mixture. Allopurinol verifies two maxima at different height. The solubility parameter values at the peaks are $\delta_1 = 32.98 \text{ MPa}^{1/2}$ and $18.49 \text{ MPa}^{1/2}$ in 70 % ethanol (1)–water (2) and in 100 % ethyl acetate (1)–ethanol (2), respectively (Tables 3, 4 and Fig. 3). The profile demonstrates a “chameleonic” behavior, characterized by the appearance of two maxima at two distinct (higher and lower) polarity values. The presence of two peaks indicates that not only polarity but also the nature of the mixture influences solubility changes [24, 25]. Different kinds of solubility profiles were reported for drugs within the wide polarity range provided by combination of dioxane–water, ethanol–water, or ethanol–ethyl acetate mixtures (Table 6). Curves with two maxima were related to more polar drugs having larger solubility

Table 3 Mole fraction solubility of allopurinol (3) in ethanol (1)+ water (2) mixtures at several temperatures and local atmospheric pressure of 950 hPa^a

Mass fraction of ethanol (1)	Study temperature range				
	288.15 K	293.15 K	298.15 K	303.15 K	308.15 K
w_1					
0.00	5.02×10^{-5} (1.35)	6.67×10^{-5} (0.8)	8.08×10^{-5} (1.28)	1.09×10^{-4} (0.49)	1.18×10^{-4} (1.96)
0.10	6.66×10^{-5} (0.93)	8.64×10^{-5} (1.93)	1.17×10^{-4} (1.04)	1.43×10^{-4} (2.78)	1.65×10^{-4} (0.73)
0.20	9.37×10^{-5} (1.65)	1.12×10^{-4} (5.13)	1.71×10^{-4} (1.34)	2.00×10^{-4} (0.65)	2.40×10^{-4} (0.36)
0.30	1.48×10^{-4} (3.32)	1.74×10^{-4} (1.69)	2.55×10^{-4} (0.84)	3.15×10^{-4} (1.62)	3.57×10^{-4} (0.23)
0.40	2.36×10^{-4} (1.22)	2.92×10^{-4} (2.06)	3.94×10^{-4} (1.53)	4.86×10^{-4} (2.05)	5.40×10^{-4} (1.55)
0.50	3.31×10^{-4} (1.59)	4.35×10^{-4} (3.07)	5.34×10^{-4} (1.47)	6.10×10^{-4} (2.25)	6.96×10^{-4} (3.47)
0.60	3.92×10^{-4} (0.91)	5.09×10^{-4} (0.7)	6.01×10^{-4} (3.98)	6.98×10^{-4} (2.18)	7.60×10^{-4} (1.92)
0.70	4.37×10^{-4} (0.86)	5.45×10^{-4} (0.42)	6.40×10^{-4} (1.92)	7.48×10^{-4} (1.4)	8.99×10^{-4} (2.54)
0.80	3.59×10^{-4} (1.4)	4.47×10^{-4} (0.37)	5.42×10^{-4} (0.17)	6.53×10^{-4} (0.64)	7.55×10^{-4} (0.78)
0.90	2.85×10^{-4} (2.44)	3.19×10^{-4} (0.47)	3.42×10^{-4} (1.83)	3.68×10^{-4} (1.06)	4.01×10^{-4} (0.65)
1.00	1.18×10^{-4} (1.99)	1.45×10^{-4} (0.32)	1.79×10^{-4} (0.86)	2.22×10^{-4} (0.83)	2.47×10^{-4} (0.53)

w_1 is the mass fraction of ethanol (1) in the ethanol (1)+water (2) mixtures free of allopurinol (3). ^a Coefficient of variation, $[CV = SD \cdot X_2 / X_{2mean}] \times 100$] in parentheses

parameter values. Solubility profiles with a single peak (usually in ethanol–ethyl acetate) were related to less polar drugs with lower solubility parameters.

3.3 Apparent Enthalpy of Solution Changes as Related to Solvent Composition

The solubilities of drug follow a linear van't Hoff relation with temperature $[\ln X_2 \text{ vs. } (1/T - 1/T_{hm})]$, at the temperature range studied (15 °C–35 °C); the correlation coefficient (r^2) for all the fits was over 0.98. The apparent molar enthalpies of solution (ΔH_2^S) are endothermic in all proportions studied. Figure 4 demonstrates non-linear relationships. Positive Gibbs energy values were obtained that diminish as the drug solubility increases. The ΔH_2^S values increase from 0 % to 20 % ethanol showing a maximum. Since the solubility also increases at this polarity region (Fig. 3), the co-solvent action must be due to favorable entropy changes related to the disruption of the ice-like water structure around the solute. Above 20 % ethanol ΔH_2^S lowers and the solubility enhancement is enthalpy-driven at this polarity region (Tables 7, 8, 9). The solubility parameter of allopurinol is 33.9 MPa^{1/2} indicating that the balance of

Table 4 Mole fraction solubility of allopurinol (3) in ethyl acetate (1)+ethanol (2) mixtures at several temperatures and local atmospheric pressure of 950 hPa^a

Mass fraction ethyl acetate (1)	Study temperature range				
	288.15 K	293.15 K	298.15 K	303.15 K	308.15 K
w_1					
0.00	1.18×10^{-4} (1.99)	1.45×10^{-4} (0.32)	1.79×10^{-4} (0.86)	2.22×10^{-4} (0.83)	2.47×10^{-4} (0.53)
0.10	3.53×10^{-4} (0.65)	3.93×10^{-4} (1.17)	4.42×10^{-4} (0.19)	4.80×10^{-4} (0.86)	5.13×10^{-4} (1.64)
0.20	4.14×10^{-4} (3.93)	5.06×10^{-4} (3.59)	5.93×10^{-4} (1.3)	6.76×10^{-4} (1.32)	7.77×10^{-4} (0.16)
0.30	6.16×10^{-4} (2.25)	6.84×10^{-4} (0.53)	8.06×10^{-4} (0.59)	9.37×10^{-4} (3.11)	1.08×10^{-3} (0.13)
0.40	9.90×10^{-4} (2.19)	1.08×10^{-3} (1.45)	1.23×10^{-3} (1.63)	1.45×10^{-3} (1.45)	1.60×10^{-3} (1.71)
0.50	1.10×10^{-3} (0.58)	1.22×10^{-3} (1.02)	1.32×10^{-3} (1.29)	1.43×10^{-3} (0.71)	1.60×10^{-3} (0.67)
0.60	1.58×10^{-3} (1.38)	1.67×10^{-3} (1.67)	1.78×10^{-3} (0.83)	1.90×10^{-3} (0.322)	2.02×10^{-3} (0.68)
0.70	1.85×10^{-3} (0.62)	1.99×10^{-3} (0.58)	2.08×10^{-3} (1.01)	2.19×10^{-3} (0.57)	2.37×10^{-3} (0.99)
0.80	2.12×10^{-3} 0.82	2.22×10^{-3} (2.04)	2.36×10^{-3} (0.44)	2.48×10^{-3} (0.33)	2.68×10^{-3} (0.12)
0.90	2.29×10^{-3} 0.30	2.48×10^{-3} (0.2)	2.64×10^{-3} (0.12)	2.78×10^{-3} (0.24)	2.97×10^{-3} (0.17)
1.00	2.81×10^{-3} (1.26)	3.05×10^{-3} (1.27)	3.23×10^{-3} (1.11)	3.48×10^{-3} (0.46)	3.70×10^{-3} (0.61)

w_1 is the mass fraction of ethyl acetate (1) in the ethyl acetate (1)+ethanol (2) mixtures free of allopurinol (3). ^a Coefficient of variation, $[CV = SD \cdot X_2 / X_{2mean}] \times 100$] in parentheses

Table 5 Mole fraction solubility of allopurinol (3) in hexane (1)+ethyl acetate (2) mixtures at several temperatures and local atmospheric pressure of 950 hPa^a

Mass fraction hexane (1)	Study temperature range				
	288.15 K	293.15 K	298.15 K	303.15 K	308.15 K
w_1					
0.00	2.81×10^{-3} (1.26)	3.05×10^{-3} (1.27)	3.23×10^{-3} (1.11)	3.48×10^{-3} (0.46)	3.70×10^{-3} (0.61)
0.20	2.16×10^{-3} (1.77)	2.32×10^{-3} (1.1)	2.51×10^{-3} (1.02)	2.66×10^{-3} (1.26)	2.84×10^{-3} (0.52)
0.30	1.94×10^{-3} (0.51)	2.05×10^{-3} (1.48)	2.17×10^{-3} (0.92)	2.31×10^{-3} (0.66)	2.47×10^{-3} (0.39)
0.50	1.57×10^{-3} (1.61)	1.71×10^{-3} (2.69)	1.82×10^{-3} (0.88)	1.95×10^{-3} (0.2)	2.08×10^{-3} (1)
0.70	1.04×10^{-3} (1.74)	1.10×10^{-3} (0.32)	1.18×10^{-3} (0.08)	1.23×10^{-3} (0.66)	1.30×10^{-3} (0.5)

w_1 is the mass fraction of hexane (1) in the hexane (1)+ethyl acetate (2) mixtures free of allopurinol (3). ^a Coefficient of variation, $[CV = SD \cdot X_2 / X_{2mean}] \times 100$] in parentheses

Table 6 Solubility parameters of different drugs

Drug	Ethanol (1) in the ethanol (1) + water (2)		Ethyl acetate (1) in the ethyl acetate (1) + ethanol (2)	
	δ_1	% ethanol	δ_1	% ethyl acetate
Sulfamethoxypyridazine [2]	30.78	80	20.90	70
Caffeine [10]	35.05	60	20.90	70
Etoricoxib [15]	–	–	20.90	70
Metronidazole [24]	30.78	80	22.50	50
Acetanilide [26]	Inflection (70 % et)		20.91	70
Benzocaine [26]	–	–	22.59	50
Phenacetine [26]	28.74	90	23.30	40
Nalidixic acid [27]	29.71	85	20.90	70
Oxolinic acid [27]	30.78	80	20.90	70
Mebendazole [28]	30.78 – 27.58	80–95	21.70	60
Acetaminophen [29]	29.71	85	24.10	30
Sulfanilamide [30]	30.78	80	21.70	60

δ_1 is the solubility parameter of the solvent ethanol (1) in the ethanol (1) + water (2) mixtures and ethyl acetate (1) in the ethyl acetate (1) + ethanol (2)

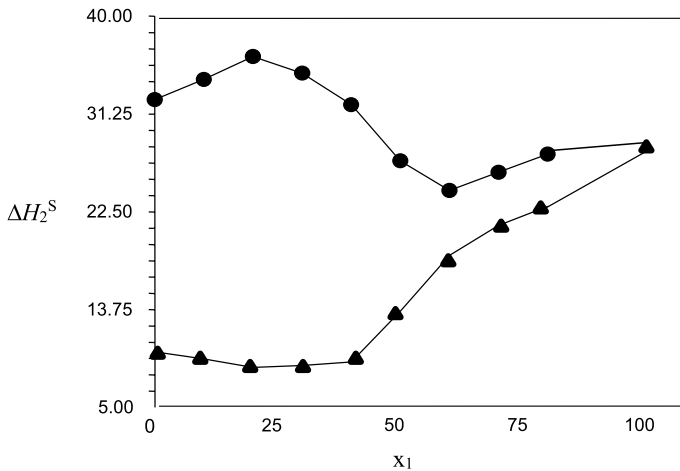


Fig. 4 ΔH_2^S (kJ·mol⁻¹) vs. volume fraction [ethanol (1) + water (2) (●) co-solvent mixtures and ethanol (1) + ethyl acetate (2) (▲) co-solvent mixtures]

non-specific interactions and cavity formation is more favorable in water. The -NH groups are capable of forming hydrogen bond with both ethanol as ethyl acetate, helping to reduce the heat of solution. Increased solubility in ethanol–ethyl acetate mixture is due to the decrease of heat of dissolution and minimum position enthalpy

Table 7 Dissolution thermodynamic quantities of allopurinol (3) in ethanol (1)+water (2) mixtures at 298.0 K

w_1	ΔG_2^S (kJ·mol ⁻¹)	ΔH_2^S (kJ·mol ⁻¹)	ΔS_2^S (J·mol ⁻¹ ·K ⁻¹)	$T \Delta S_2^S$ (kJ·mol ⁻¹)	% ζ_H	% ζ_{TS}
0.00	23.33	32.533	- 78.269	- 23.336	58.2	41.8
0.10	22.51	34.332	- 75.736	- 22.580	60.3	39.7
0.20	21.74	36.379	- 72.918	- 21.74	62.6	37.4
0.30	20.68	34.899	- 69.352	- 20.677	62.8	37.2
0.40	19.55	32.078	- 65.578	- 19.552	62.1	37.9
0.50	18.80	27.053	- 63.054	- 18.799	59.0	41.0
0.60	18.47	24.404	- 61.95	- 18.470	56.9	43.1
0.70	18.67	26.033	- 62.645	- 18.677	58.2	41.8
0.80	18.64	27.651	- 62.602	- 18.665	59.7	40.3
0.90	19.78	12.263	- 66.351	- 19.782	38.3	61.7
1.00	21.41	28.151	- 71.819	- 21.412	56.8	43.2

w_1 is the mass fraction of ethanol (1) in the ethanol(1) + water (2) mixtures free of allopurinol (3). ΔG_2^S is Gibbs energy of solution, ΔH_2^S is enthalpy of solution, ΔS_2^S is entropy of solution. % ζ_H and % ζ_{TS} represent the relative contributions of the enthalpy and entropy

Table 8 Dissolution thermodynamic quantities of allopurinol (3) in ethyl acetate (1) + ethanol (2) mixtures at 298.0 K

w_1	ΔG_2^S (kJ·mol ⁻¹)	ΔH_2^S (kJ·mol ⁻¹)	ΔS_2^S (J·mol ⁻¹ K ⁻¹)	$T \Delta S_2^S$ (kJ·mol ⁻¹)	% ζ_H	% ζ_{TS}
0.00	21.41	28.151	- 71.819	- 21.412	56.8	43.2
0.10	19.19	13.995	- 64.366	- 19.190	42.2	57.9
0.20	18.45	22.975	- 61.914	- 18.459	55.5	44.6
0.30	17.63	21.267	- 59.152	- 17.636	54.7	45.3
0.40	16.55	18.601	- 55.507	- 16.549	53.0	47.1
0.50	16.41	13.588	- 55.052	- 16.413	45.3	54.7
0.60	15.67	9.0683	- 52.566	- 15.672	36.7	63.3
0.70	15.28	8.7520	- 51.253	- 15.281	36.4	63.6
0.80	14.97	8.5712	- 50.231	- 14.976	36.4	63.6
0.90	14.71	9.3512	- 49.355	- 14.715	38.9	61.1
1.00	14.19	9.9612	- 47.595	- 14.190	41.2	58.8

w_1 is the mass fraction of ethyl acetate (1) in the ethyl acetate (1) + ethanol (2) mixtures free of allopurinol (3). ΔG_2^S is Gibbs energy solution, ΔH_2^S is enthalpy of solution, ΔS_2^S is entropy of solution. % ζ_H and % ζ_{TS} represent the relative contributions of the enthalpy and entropy

Table 9 Dissolution thermodynamic quantities of allopurinol (3) in hexane (1)+ethyl acetate (2) mixtures at 298.0 K

w_1	ΔG_2^S (kJ·mol ⁻¹)	ΔH_2^S (kJ·mol ⁻¹)	ΔS_2^S (J·mol ⁻¹ K ⁻¹)	$T\Delta S_2^S$ (kJ·mol ⁻¹)	% ξ_H	% ξ_{TS}
0.00	14.19	9.9612	- 47.595	- 14.190	41.3	58.8
0.20	14.84	10.074	- 49.801	- 14.848	40.4	59.6
0.30	15.17	8.9770	- 50.912	- 15.179	37.2	62.9
0.50	15.63	10.218	- 52.433	- 15.632	39.6	60.5
0.70	16.73	8.2674	- 56.116	- 16.731	66.0	34.0

w_1 is the mass fraction of hexane (1) in the hexane (1)+ethyl acetate (2) mixtures free of allopurinol (3). ΔG_2^S is Gibbs energy solution, ΔH_2^S is enthalpy of solution, ΔS_2^S is entropy of solution. % ξ_H and % ξ_{TS} represent the relative contributions of the enthalpy and entropy

solute dependent. While the increase in solubility in the aqueous mixture is due to the decrease in the hydrophobic effect, the entropy increases.

The relative contributions of the enthalpy (% ξ_H) and entropy (% ξ_{TS}) to the process of dissolution were evaluated using the Eqs. 2 and 3 [31] (Tables 7, 8, 9).

$$\% \xi_H = \frac{|\Delta H_2^S|}{|\Delta H_2^S| + |T\Delta S_2^S|} \cdot 100 \quad (2)$$

$$\% \xi_{TS} = \frac{|T\Delta S_2^S|}{|\Delta H_2^S| + |T\Delta S_2^S|} \cdot 100 \quad (3)$$

where T is the temperature of work at 298.0 K, ΔG_2^S is the Gibbs energy of solution, ΔH_2^S is the enthalpy of solution, and ΔS_2^S is the entropy of solution.

% ξ_H and % ξ_{TS} represent the relative contributions of the enthalpy and entropy to the dissolution, respectively, to express the participation of each magnitude in the process. The highest contribution of the enthalpy was produced at 70 % of hexane in ethyl acetate–hexane mixtures, while the maximum contribution of the entropy was at 70 % of ethyl acetate in ethanol–ethyl acetate mixtures.

3.4 Enthalpy–Entropy Relationship

The enthalpy–entropy compensation is tested to corroborate the mechanism of the co-solvent action. The compensation plots obtained in the ΔH_2^S – ΔG_2^S plane for ethanol–water mixtures are parabolic (Table 10 and Fig. 5). The positive slope of the parabola corresponds to the ethanol-rich region (lower ΔG_2^S values) and the negative slope to the water-rich region (higher ΔG_2^S values). The parabola is a symmetrical open plane curve formed by the intersection of a cone with a plane parallel to its

Table 10 Gibbs energy of transfer ($\Delta_{tr}G_{3,2 \rightarrow 1+2}/\text{kJ}\cdot\text{mol}^{-1}$) of allopurinol (3) from solvent (2) to solvent (1) + solvent (2) mixtures at several temperatures

Ethanol (1) + water (2)				Ethyl acetate (1) + ethanol (2)			
x_1^a	298.15 K	303.5 K	308.15 K	x_1^b	298.15 K	303.5 K	308.15 K
0.0000	0.00	0.00	0.00	0.0000	0.00	0.00	0.00
0.0417	-0.63	-0.91	-0.70	0.0549	-2.47	-2.27	-1.97
0.0891	-1.27	-1.85	-1.54	0.1156	-3.10	-3.02	-2.85
0.1436	-2.34	-2.85	-2.69	0.1831	-3.85	-3.79	-3.69
0.2068	-3.60	-3.93	-3.78	0.2585	-4.98	-4.86	-4.81
0.2812	-4.57	-4.68	-4.35	0.3434	-5.29	-5.03	-4.77
0.3698	-4.95	-4.97	-4.69	0.4396	-6.06	-5.79	-5.50
0.4772	-5.12	-5.13	-4.86	0.5496	-6.50	-6.18	-5.87
0.6101	-4.64	-4.72	-4.52	0.6765	-6.77	-6.49	-6.18
0.7788	-3.82	-3.57	-3.08	0.8247	-7.04	-6.78	-6.47
1.0000	-1.89	-1.97	-1.81	1.0000	-7.55	-7.29	-7.05

^a x_1 is the mole fraction of ethanol (1) in ethanol (1) + water (2) free of allopurinol (3)

^b x_1 is the mole fraction of ethyl acetate (1) in ethyl acetate (1) + ethanol (2) free of allopurinol (3)

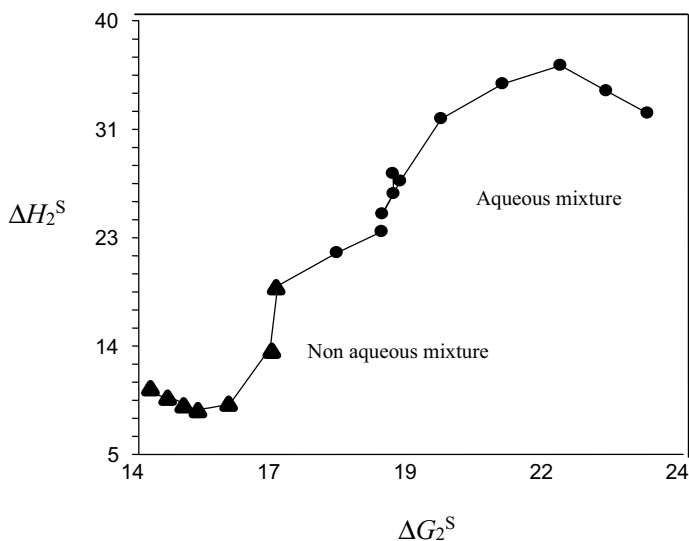


Fig. 5 ΔH_2^S ($\text{kJ}\cdot\text{mol}^{-1}$) vs. ΔG_2^S ($\text{kJ}\cdot\text{mol}^{-1}$) enthalpy–entropy compensation plot for allopurinol [ethanol (1) + water (2) (\square) co-solvent mixtures and ethanol (1) + ethyl acetate (2) (\blacktriangle) co-solvent mixtures]

side. The maximum of each parabolic relationship separates the dominant mechanism, enthalpy (left branch), and entropy (right branch).

In Figure 5, the slope is negative in the water-rich region and positive in the ethanol-rich region (right and left around the maximum located in 20 % ethanol). The shift of the slope reveals a change in mechanism from a (positive slope, low

values of ΔG_2^S) to entropic component (negative slope to higher values ΔG_2^S) enthalpic component. In the mixture of ethanol and ethyl acetate, two different relationships are produced, with a change in slope from positive to negative, corresponding to enthalpy and entropy.

3.5 The Jouyban–Acree Model

The Jouyban–Acree model provides more accurate mathematical descriptions and shows how a solute solubility varies with both temperature and solvent composition. The general form of this model for representing a solute solubility in binary solvent mixtures is shown as Jouyban [3]:

$$\ln X_{m,T}^{Sat} = m_1 \cdot \ln X_{1,T}^{Sat} + m_2 \cdot \ln X_{2,T}^{Sat} + \frac{m_1 \cdot m_2}{T} \cdot \sum_{i=0}^2 J_i \cdot (m_1 - m_2)^i \quad (4)$$

where $X_{m,T}^{Sat}$ is the solute mole fraction solubility in the mixture at temperature T ; m_1 and m_2 are the mass fractions of solvents 1 and 2 in the absence of the solute; $X_{1,T}^{Sat}$ and $X_{2,T}^{Sat}$ denote the mole fraction solubility of the solute in the mono-solvents 1 and 2; and J_i terms are the constants of the model computed by a regression analysis.

Solubility at different temperatures ($\ln X_T^{Sat}$) could be calculated using the van't Hoff equation presented as [32]:

$$\ln X_T^{Sat} = A + \frac{B}{T} \quad (5)$$

where A and B are the model constants calculated using a least square method. Combination of the Jouyban–Acree and van't Hoff model enables the prediction of drug solubility in mixed solvents at different temperatures after training process using two solubility data points, e.g., at the lowest and highest temperatures for each solvent [4, 33]. The combined version could be represented as:

$$\ln X_T^{Sat} = m_1 \left(A_1 + \frac{B_1}{T} \right) + m_2 \left(A_2 + \frac{B_2}{T} \right) + \frac{m_1 \cdot m_2}{T} \cdot \sum_{i=0}^2 J_i \cdot (m_1 - m_2)^i \quad (6)$$

where A_1 , B_1 , A_2 , B_2 , and J_i terms are the model constants.

Equation (4) could be used to compute the solute solubility in ternary solvent mixtures as [3].

$$\begin{aligned} \ln X_{m,T}^{Sat} = & m_1 \ln X_{1,T}^{Sat} + m_2 \ln X_{2,T}^{Sat} + m_3 \ln X_{3,T}^{Sat} + \left[\frac{m_1 m_2}{T} \sum_{i=0}^2 J_i (m_1 - m_2)^i \right] + \\ & \left[\frac{m_1 m_3}{T} \sum_{i=0}^2 J'_i (m_1 - m_3)^i \right] + \left[\frac{m_2 m_3}{T} \sum_{i=0}^2 J''_i (m_2 - m_3)^i \right] \end{aligned} \quad (7)$$

in which $X_{3,T}^{Sat}$ and m_3 terms are the solubility of solute in mono-solvent 3 and mass fraction of solvent 3, respectively. The J_i constants of Eq. 7 could be calculated by

using the above-mentioned method. It could also be extended for quaternary solvent mixtures as:

$$\begin{aligned} \ln X_{m,T}^{Sat} = & m_1 \ln X_{1,T}^{Sat} + m_2 \ln X_{2,T}^{Sat} + m_3 \ln X_{3,T}^{Sat} + m_4 \ln X_{4,T}^{Sat} + \left[\frac{m_1 m_2}{T} \sum_{i=0}^2 J_i (m_1 - m_2)^i \right] + \\ & \left[\frac{m_1 m_3}{T} \sum_{i=0}^2 J'_i (m_1 - m_3)^i \right] + \left[\frac{m_1 m_4}{T} \sum_{i=0}^2 J''_i (m_1 - m_4)^i \right] + \left[\frac{m_2 m_3}{T} \sum_{i=0}^2 J'''_i (m_2 - m_3)^i \right] \\ & + \left[\frac{m_2 m_4}{T} \sum_{i=0}^2 J''''_i (m_2 - m_4)^i \right] + \left[\frac{m_3 m_4}{T} \sum_{i=0}^2 J'''''_i (m_3 - m_4)^i \right] \end{aligned} \quad (8)$$

It is possible to calculate the J terms at one temperature and predict the solubility of a solute at other temperatures [32]. Prediction of the solubility in the mixed solvents at various temperatures, with a trained Jouyban–Acree model, needs a number of experimental solubility data in mono-solvents that it can be considered as a limitation of the Jouyban–Acree model. A combination of Eq. 5 with Eq. 8 yields:

$$\begin{aligned} \ln X_{m,T}^{Sat} = & m_1 \left(A_1 + \frac{B_1}{T} \right) + m_2 \left(A_2 + \frac{B_2}{T} \right) + m_3 \left(A_3 + \frac{B_3}{T} \right) + m_4 \left(A_4 + \frac{B_4}{T} \right) \\ & + \left[\frac{m_1 m_2}{T} \sum_{i=0}^2 J_i (m_1 - m_2)^i \right] + \left[\frac{m_1 m_3}{T} \sum_{i=0}^2 J'_i (m_1 - m_3)^i \right] + \left[\frac{m_1 m_4}{T} \sum_{i=0}^2 J''_i (m_1 - m_4)^i \right] \\ & + \left[\frac{m_2 m_3}{T} \sum_{i=0}^2 J'''_i (m_2 - m_3)^i \right] + \left[\frac{m_2 m_4}{T} \sum_{i=0}^2 J''''_i (m_2 - m_4)^i \right] + \left[\frac{m_3 m_4}{T} \sum_{i=0}^2 J'''''_i (m_3 - m_4)^i \right] \end{aligned} \quad (9)$$

To check the validity of the model in predicted solubility values, a comparison is made between calculated ($C_{Calculated}^{Sat}$) and experimental solubility ($C_{Experimental}^{Sat}$) values by the mean percentage deviation (MPD) by the following formula:

$$MPD = \frac{100}{N} \sum \left(\frac{\left| C_{Calculated}^{Sat} - C_{Experimental}^{Sat} \right|}{C_{Experimental}^{Sat}} \right) \quad (10)$$

in which N is the number of data points in each set.

When the solubility data were fitted to Eq. 9, the trained model was:

$$\begin{aligned}
\ln X_{m,T}^{Sat} = & m_1 \left(5.756 - \frac{4520.199}{T} \right) + m_2 \left(0.895 - \frac{2828.908}{T} \right) \\
& + m_3 \left(-2.514 - \frac{967.507}{T} \right) + m_4 \left(-2.937 - \frac{1570.567}{T} \right) \\
& + \frac{m_1 m_2}{T} \left[1668.834 - 1103.366(m_1 - m_2) - 253.463(m_1 - m_2)^2 \right] \quad (11) \\
& + \frac{m_2 m_3}{T} \left[737.741 + 549.827(m_2 - m_3) + 364.407(m_2 - m_3)^2 \right] \\
& + \frac{m_3 m_4}{T} \left[789.175 - 590.370(m_3 - m_4) \right]
\end{aligned}$$

where solvents 1 to 4 were defined as water, ethanol, ethyl acetate, and n-hexane (m), respectively. Equation (11) back-calculates the solubility data with the overall % deviation of 5.1 ± 4.3 %.

3.6 Preferential Solvation

The preferential solvation parameter of allopurinol (component 3) in ethanol (1) + water (2) or ethyl acetate (1) + ethanol (2) mixtures is defined as:

$$\delta x_{1,3} = x_{1,3}^L - x_1 = \delta x_{2,3} \quad (12)$$

where $x_{1,3}^L$ is the local mole fraction of solvent (1) in the environment near to allopurinol (3) and x_1 is the bulk mole fraction of ethanol in the initial aqueous co-solvent mixture in the absence of allopurinol or the bulk mole fraction of ethyl acetate in the initial non-aqueous co-solvent mixture in the absence of allopurinol.

If $\delta x_{1,3} > 0$, then the drug is preferentially solvated by solvent (1); on the contrary, if this parameter is < 0 , the drug is preferentially solvated by solvent (2). Values of $\delta x_{1,3}$ are obtainable from the inverse Kirkwood–Buff integrals for the individual solvent components analyzed in terms of some thermodynamic quantities as shown in the following equations [34, 35]:

$$G_{1,3} = RT\kappa_T - V_3 + x_2 V_2 D/Q \quad (13)$$

$$G_{2,3} = RT\kappa_T - V_3 + x_1 V_1 D/Q \quad (14)$$

where κ_T is the isothermal compressibility of the solvent (1) + solvent (2) solvent mixtures (in GPa^{-1}); V_1 and V_2 are the partial molar volumes of the solvents in the mixtures; similarly, V_3 is the partial molar volume of allopurinol (3) in these mixtures (in $\text{cm}^3 \text{mol}^{-1}$). The function D is defined as the derivative of the standard molar Gibbs energies of transfer of the drug (from neat solvent (2) to solvent (1) + solvent (2) mixtures) with respect to the solvent composition (in $\text{kJ}\cdot\text{mol}^{-1}$, as also is RT) and the function Q involves the second derivative of the excess molar Gibbs energy of mixing of the two solvents (G_{1+2}^{Exc}) with respect to the water proportion in the mixtures (also in $\text{kJ}\cdot\text{mol}^{-1}$) [34, 35]:

$$D = \left(\frac{\partial \Delta_{\text{tr}} G_{3,2 \rightarrow 1+2}^0}{\partial x_1} \right)_{T,p} \quad (15)$$

$$Q = RT + x_1 x_2 \left(\frac{\partial^2 G_{1+2}^{\text{Exc}}}{\partial x_2^2} \right)_{T,p} \quad (16)$$

Because the dependence of κ_T on composition is not known for a lot of the systems investigated and because of the small contribution of $RT \kappa_T$ to the inverse Kirkwood–Buff integrals (IKBI), the dependence of κ_T on composition [36] could be approximated by considering the additive behavior according to:

$$\kappa_{T,\text{mix}} = \sum_{i=1}^n x_i \kappa_{T,i}^0 \quad (17)$$

where x_i is the mole fraction of component i in the mixture and $\kappa_{T,i}^0$ is the isothermal compressibility of the pure component i [29]. Therefore, the preferential solvation parameter can be calculated from the Kirkwood–Buff integrals as follows:

$$\delta x_{1,3} = \frac{x_1 x_3 (G_{1,3} - G_{2,3})}{x_1 G_{1,3} + x_2 G_{2,3} + V_{\text{cor}}} \quad (18)$$

here the correlation volume (V_{cor}) is obtained by means of the following expression [34, 35]:

$$V_{\text{cor}} = \frac{x_1 x_3 (G_{1,3} - G_{2,3})}{x_1 G_{1,3} + x_2 G_{2,3} + V_{\text{cor}}} \quad (19)$$

where r_3 is the radius value of allopurinol (in nm). However, the definitive correlation volume requires iteration, because it depends on the local mole fractions. This iteration is done by replacing $\delta x_{1,3}$ in the Eq. 12 to calculate $x_{1,3}^L$ until a non-variant value of V_{cor} is obtained.

Table 10 shows the Gibbs energy of transfer behavior of allopurinol (3) from neat solvent (2) to solvent (1)+solvent (2) mixtures at several temperatures. These values were calculated and correlated according to the polynomial presented as Eq. 20 from the drug solubility data reported in Tables 3, 4, and 5.

$$\Delta_{\text{tr}} G_{3,2 \rightarrow 1+2}^0 = RT \ln \left(\frac{x_{3,2}}{x_{3,1+2}} \right) = a + bx_1 + cx_1^2 + dx_1^3 + ex_1^4 \quad (20)$$

Thus, D values were calculated from the first derivative of the polynomial model solved according to the solvent mixtures composition. Otherwise, the Q and $RT \kappa_T$ values, as well as the partial molar volumes of solvents in the mixtures for ethanol (1)+water (2) and ethyl acetate (1)+ethanol (2) mixtures, were taken from the references Rodríguez [36] and Delgado [37], respectively. On the other hand, the partial molar volumes of non-dissociate weak electrolyte drugs such as allopurinol

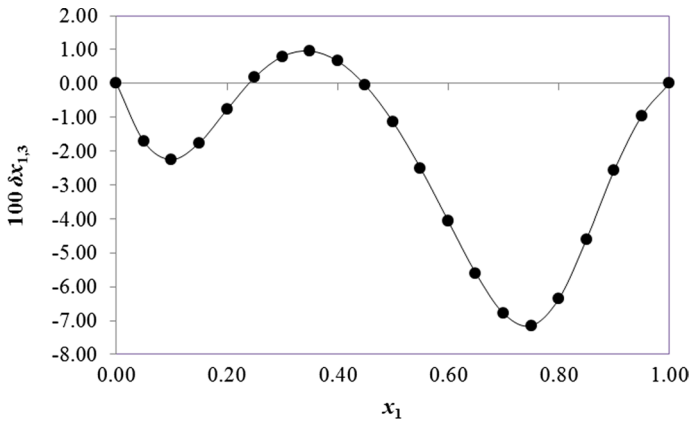


Fig. 6 Preferential solvation parameter of allopurinol by ethanol (1) in ethanol (1)+water (2) solvent mixtures at 298.15 K

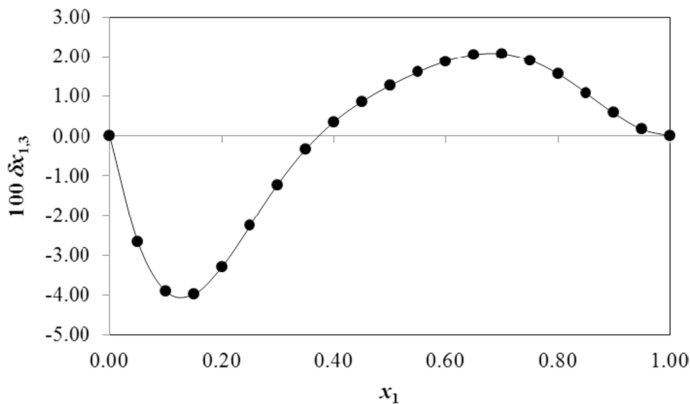


Fig. 7 Preferential solvation parameter of allopurinol by ethyl acetate (1) in ethyl acetate (1)+ethanol (2) solvent mixtures at 298.15 K

is not frequently reported in the literature. This is because of the big uncertainty obtained in its determination due to the low solubilities exhibited by them, particularly in aqueous media [38–41]. For this reason, in a first approach, the molar volume of allopurinol is considered here as independent of co-solvent composition, as it is calculated according to the groups contribution method proposed by Fedors [42] as $71.2 \text{ cm}^3 \cdot \text{mol}^{-1}$. Otherwise, allopurinol radius value (r_3) is required to calculate the correlation volume and was calculated from the molar volume as 0.304 nm . According to Figs. 6 and 7 (Table 11), the values of $\delta x_{1,3}$ vary non-linearly with the ethanol proportion in all the mixtures exhibiting negative and positive values. Addition of ethanol (1) to water (2) tends to make negative the preferential solvation values, $\delta x_{1,3}$ of this drug, from the pure water (2) up to the mixture 0.24 in mole fraction of ethanol (1) reaching minimum values near to -2.06×10^{-2} in the mixture

Table 11 Preferential solvation parameters of allopurinol ($\delta x_{1,3}$) by the solvent (1) in the solvent (1) + solvent (2) mixtures at several temperatures

Ethanol (1) + water (2)				Ethyl acetate (1) + ethanol (2)			
x_1^a	298.15 K	303.5 K	308.15 K	x_1^b	298.15 K	303.5 K	308.15 K
0.00	0.000	0.000	0.000	0.00	0.000	0.000	0.000
0.10	-2.056	-2.246	-2.154	0.10	-3.912	-3.724	-3.565
0.20	-0.830	-0.771	-0.782	0.20	-3.292	-2.972	-2.764
0.30	0.996	0.796	0.850	0.30	-1.227	-1.049	-0.936
0.40	1.264	0.661	0.671	0.40	0.346	0.293	0.253
0.50	-0.540	-1.135	-1.296	0.50	1.263	1.099	0.913
0.60	-4.027	-4.062	-4.423	0.60	1.873	1.773	1.525
0.70	-7.462	-6.786	-7.237	0.70	2.072	2.091	1.920
0.80	-7.109	-6.355	-6.498	0.80	1.556	1.611	1.606
0.90	-2.815	-2.570	-2.168	0.90	0.575	0.581	0.678
1.00	0.000	0.000	0.000	1.00	0.000	0.000	0.000

^a x_1 is the mole fraction of ethanol (1) in ethanol (1) + water (2) free of allopurinol (3)

^b x_1 is the mole fraction of ethyl acetate (1) in ethyl acetate (1) + ethanol (2) free of allopurinol (3)

with 0.10 in mole fraction of ethanol (1) at 298.15 K. Possibly the structuring of water molecules around the non-polar groups of the drug (aromatic rings, Fig. 1) by hydrophobic hydration contributes to lowering of the net $\delta x_{1,3}$ to negative values in these water-rich mixtures.

In the mixtures with composition $0.30 < x_1 < 0.45$, the local mole fractions of ethanol (1) are greater than the ones for water (2). In this way, the co-solvent action may be related to the breaking of the ordered structure of water by hydrogen bonding around the non-polar moieties of the drug, as was appointed previously. Finally, in compositions with $0.50 < x_1 < 1.00$, the $\delta x_{1,3}$ values are negative again, being the drug preferentially solvated by water. Figure 6 shows that the values of $\delta x_{1,3}$ vary non-linearly with the ethanol proportion in the aqueous mixtures. Addition of ethanol to water tends to make negative the $\delta x_{1,3}$ values of this drug from the pure water up to the mixture $x_1 = 0.25$ reaching a minimum value in the mixture $x_1 = 0.10$. Possibly the hydrophobic hydration around the non-polar groups of drug contributes to lowering of the net $\delta x_{1,3}$ to negative values in these water-rich mixtures. In the mixtures with composition $0.25 < x_1 < 0.45$, the local mole fraction of ethanol is greater than one for water. In this way, the co-solvent action may be related to the breaking of the ordered structure of water (hydrogen bonds) around the non-polar moieties of the drug which increases the solvation of drug and exhibits a maximum value in $x_1 = 0.35$. Ultimately, from this ethanol proportion up to neat ethanol, the $\delta x_{1,3}$ values are negative again.

It is conjecturable that, in $0.25 < x_1 < 0.45$ region, drug is acting as Lewis acid with ethanol molecules because this co-solvent is more basic than water, *i.e.*, the Kamlet–Taft hydrogen bond acceptor parameters are $\beta = 0.75$ for ethanol and 0.47 for water [43]. On the other hand, in ethanol-rich mixtures, where the drug is preferentially solvated by water, the drug is acting mainly as a Lewis base in front

to water because the Kamlet–Taft hydrogen bond donor parameters are $\alpha = 1.17$ for water and 0.86 for ethanol, respectively [43]. Figure 7 illustrates the preferential solvation parameters of allopurinol (3) by EtOAc (1) at 298.15 K. The values of $\delta x_{1,3}$ vary non-linearly with the EtOAc (1) proportion in these organic mixtures. Addition of EtOAc (1) to EtOH (2) makes the $\delta x_{1,3}$ values of this drug from the pure EtOH (2) to the mixture 0.37 in mole fraction of EtOAc (1) negative, reaching a minimum in the mixture with 0.15 in mole fraction of EtOAc (1).

In the mixtures with compositions $0.37 < x_1 < 1.00$, the local mole fractions of EtOAc (1) are higher than the mole fraction of EtOAc (1) in the mixtures. Thus, the solvent action may be related to the breaking of the slightly ordered structure of ethanol molecules, which are joined by hydrogen bonding of its hydroxyl groups. Allopurinol could act in solution as a Lewis acid (owing to its $>NH$ groups, Fig. 1) to establish hydrogen bonds with proton-acceptor functional groups in the solvents (oxygen atoms in $-OH$ or $>C=O$ or $-O-$ groups). This drug could also act as a proton-acceptor compound by means of free electrons in its oxygen atom in $>C=O$ groups and its nitrogen atoms (Fig. 1) to interact with the hydrogen atoms of EtOH (2). Thus, it is possible that in mixtures with an intermediate composition and EtOAc-rich mixtures, allopurinol (3) is acting as a Lewis acid with the EtOAc (1) molecules even when this organic solvent is less basic than EtOH, as described by the respective Kamlet–Taft hydrogen bond acceptor parameters, i.e., $\beta = 0.45$ for EtOAc and 0.75 for EtOH (2); nevertheless, polarizability effects could also be involved.

4 Conclusion

Equilibrium solubility of allopurinol was determined in water–ethanol and ethanol–ethyl acetate co-solvent mixtures at 15 °C–35 °C. Solubility profile showed initial rising curve followed by a second peak higher (70 % ethanol–water and 100 % ethyl acetate). The solid phases of allopurinol not experience any change after equilibration with the different pure solvents and binary solvent mixtures examined.

The thermodynamic findings obtained support that the entropic effect of the medium is the origin of the co-solvent action in aqueous mixtures at the water-rich region. At higher ethanol in water ratios, the favorable enthalpy changes, related to solute–solvent interactions, are the origin of the co-solvent action. The drug shows parabolic enthalpy–entropy compensation patterns. The maxima or the minimum separates the dominant mechanism that controls the co-solvent action. Moreover, IKBI model has been used to evaluate the preferential solvation of that drug by solvent components of the mixtures. Thus, allopurinol is preferentially solvated by water in water-rich mixtures and also in ethanol-rich mixtures but preferentially solvated by ethanol in mixtures with intermediate composition.

Supplementary Information The online version contains supplementary material available at <https://doi.org/10.1007/s10765-022-03061-6>.

Funding Open Access funding provided thanks to the CRUE-CSIC agreement with Springer Nature.

Declarations

Conflict of interest No potential conflict of interest was reported by the authors.

Open Access This article is licensed under a Creative Commons Attribution 4.0 International License, which permits use, sharing, adaptation, distribution and reproduction in any medium or format, as long as you give appropriate credit to the original author(s) and the source, provide a link to the Creative Commons licence, and indicate if changes were made. The images or other third party material in this article are included in the article's Creative Commons licence, unless indicated otherwise in a credit line to the material. If material is not included in the article's Creative Commons licence and your intended use is not permitted by statutory regulation or exceeds the permitted use, you will need to obtain permission directly from the copyright holder. To view a copy of this licence, visit <http://creativecommons.org/licenses/by/4.0/>.

References

1. P. Bustamante, B. Escalera, A. Martin, E. Sellés, *J. Pharm. Pharmacol.* **45**, 253 (1993)
2. B. Escalera, P. Bustamante, A. Martin, *J. Pharm. Pharmacol.* **46**, 172 (1994)
3. A. Jouyban, *J. Pharm. Pharm. Sci.* **11**, 32 (2008)
4. A. Jouyban, A. Shayanfar, W.E. Acree, *Fluid Phase Equilib.* **293**, 47–58 (2010)
5. A. Jouyban, *Handbook Solubility Data for Pharmaceuticals* (CRC Press, Boca Raton, Florida, 2010)
6. F. Martinez, A. Jouyban, W. Acree, *Pharm. Sci.* **23**, 1 (2017)
7. E. Mohammadian, E. Rahimpour, F. Martinez, A. Joyuban, *Phys. Chem. Liq.* **56**, 751 (2018)
8. F. Saadatfar, A. Shayanfar, E. Rahimpour, M. Barzegar-Jalali, F. Martinez, M. Bolourtchian, A. Jouyban, *J. Mol. Liq.* **256**, 527 (2018)
9. A. Jouyban, W.E. Acree, F. Martínez, *J Appl Sol Chem Model.* **7**, 1 (2018)
10. S. Mirzaeei, F.H. Pirhayati, G. Mohammadi, E. Rahimpour, F. Martínez, A. Jouyban, *Phys. Chem. Liq.* **57**, 788 (2019)
11. A. Romdhani, F. Martínez, O.A. Almanza, M.A. Peña, A. Jouyban, W.E. Acree, *J. Mol. Liq.* **290**, 111219 (2019)
12. P. Bustamante, J. Navarro, S. Romero, B. Escalera, *J. Pharm. Sci.* **91**, 874 (2002)
13. M.A. Peña, B. Escalera, A. Reíllo, A.B. Sánchez, P. Bustamante, *J. Pharm. Sci.* **98**, 1129 (2009)
14. D.R. Delgado, G.A. Rodríguez, F. Martínez, *J. Mol. Liq.* **177**, 156 (2013)
15. N. Torres, B. Escalera, F. Martínez, M.A. Peña, *J. Solution Chem.* **49**, 272 (2020)
16. P. Bustamante, S. Romero, A. Peña, B. Escalera, A. Reíllo, *J. Pharm. Sci.* **87**, 1590 (1998)
17. S. Akay, B. Kayan, F. Martínez, *Phys. Chem. Liq.* **596**, 956 (2021)
18. S. Akay, B. Kayan, A. Jouyban, F. Martínez, *J. Mol. Liq.* **333**, 116038 (2021)
19. F. Shakeel, S. Alshehri, M.M. Ghoneim, F. Martínez, M.A. Peña, A. Jouyban, W.E. Acree, *Phys Chem Liq.* in press (2022)
20. W. Li, J. Yuan, X. Wang, W. Shi, H. Zhao, R. Xing, A. Jouyban, W.E. Acree Jr., *J. Mol. Liq.* **338**, 116671 (2021)
21. R.R. Krug, W.G. Hunter, R.A. Grieger, *J. Phys. Chem.* **80**(21), 2341 (1976)
22. R. Cárdenas, C. Ortiz, W.E. Acree, A. Jouyban, F. Martínez, D. Delgado, *J. Mol. Liq.* **349**, 118172 (2022)
23. M. Barzegar-Jalali, E. Haji, K. Adibkia, S. Hemmati, F. Martínez, A. Jouyban, *Phys. Chem. Liq.* **59**(5), 690 (2021)
24. P. Bustamante, S. Muela, B. Escalera, M.A. Peña, *Chem. Pharm. Bull.* **58**(5), 644 (2010)
25. M. Khoubnasabjafari, D.R. Delgado, F. Martínez, A. Jouyban, *Phys. Chem. Liq.* **59**(3), 400 (2021)
26. M.A. Peña, A. Reíllo, B. Escalera, P. Bustamante, *Int. J. Pharm.* **321**, 155 (2006)
27. S. Romero, P. Bustamante, B. Escalera, P. Mura, M. Cirri, *J. Pharm. Biomed. Anal.* **35**(4), 715 (2004)
28. S. Muela, B. Escalera, M.A. Peña, P. Bustamante, *Int. J. Pharm.* **384**, 93 (2010)
29. S. Romero, A. Reíllo, B. Escalera, P. Bustamante, *Chem. Pharm. Bull.* **44**, 1061 (1996)
30. P. Bustamante, R. Ochoa, A. Reíllo, B. Escalera, *Chem. Pharm. Bull.* **42**, 1129 (1994)

31. G.L. Perlovich, V. Kurkov, A.N. Kinchin, A. Bauer-Brandl, *Eur. J. Pharm. Biopharm.* **57**, 411 (2004)
32. D.J.W. Grant, M. Mehdizadeh, A.H.L. Chow, J.E. Fairbrother, *Int. J. Pharm.* **18**, 25 (1984)
33. A. Jouyban, M.A.A. Fakhree, W.E. Acree, *J. Chem. Eng. Data.* **57**(4), 1344 (2012)
34. Y. Marcus, *J. Mol. Liq.* **140**, 61 (2008)
35. Y. Marcus, *Acta Chim. Sloven.* **56**, 40 (2009)
36. G.A. Rodríguez, D.R. Delgado, F. Martínez, *Phys. Chem. Liq.* **52**(4), 533 (2014)
37. D.R. Delgado, M.A. Peña, F. Martínez, *J. Solut. Chem.* **43**, 360 (2014)
38. D.R. Delgado, F. Martínez, *J. Mol. Liq.* **193**, 152 (2014)
39. S. Alshehri, F. Shakeel, P. Alam, M.A. Peña, A. Jouyban, F. Martínez, *J. Mol. Liq.* **340**, 117268 (2021)
40. M.S. Vargas, A.M. Cruz, C.P. Ortiz, D.R. Delgado, F. Martínez, M.A. Peña, W.E. Acree, A. Jouyban, *J. Mol. Liq.* **337**, 116330 (2021)
41. Z. Fang, Z. Jianhua, L. Hui, *J. Mol. Liq.* **339**, 117014 (2021)
42. R.F. Fedors, *Polym. Eng. Sci.* **14**, 147 (1974)
43. M.J. Kamlet, R.W. Taft, *J. Am. Chem. Soc.* **98**, 377 (1976)

Publisher's Note Springer Nature remains neutral with regard to jurisdictional claims in published maps and institutional affiliations.

Authors and Affiliations

M. Ángeles Peña¹  · Ana B. Sánchez¹ · Begoña Escalera¹  ·
Abolghasem Jouyban^{2,3}  · Fleming Martinez⁴ 

- ¹ Departamento de Ciencias Biomédicas, Facultad de Farmacia, Universidad de Alcalá, Alcalá de Henares, 28871 Madrid, Spain
- ² Pharmaceutical Analysis Research Center, Faculty of Pharmacy, Tabriz University of Medical Sciences, Tabriz, Iran
- ³ Faculty of Pharmacy, Near East University, Nicosia, North Cyprus, PO BOX: 99138, Mersin 10, Turkey
- ⁴ Grupo de Investigaciones Farmacéutico-Fisicoquímicas, Departamento de Farmacia, Facultad de Ciencias, Universidad Nacional de Colombia, Sede Bogotá, Cra. 30 No. 45-03, Bogotá, D. C., Colombia